



On the Paradoxical Impact of Blending by Red Clump Giants

Daniel J. Majaess^{1,2}

¹ Mount Saint Vincent University, Halifax, Nova Scotia, Canada; daniel.majaess@msvu.ca

² Saint Mary's University, Halifax, Nova Scotia, Canada

Received 2020 March 26; revised 2020 April 14; accepted 2020 April 24; published 2020 June 26

Abstract

The impact of blending by red clump giants (RCGs; or relatively metal-rich red horizontal branch stars) is discussed as it relates to RRab and classical Cepheids, and invariably establishing an improved distance scale. An analysis of Magellanic Cloud variables reaffirms that blending with RCGs may advantageously thrust remote extragalactic stars into the range of detectability. Specifically, simulations of Magellanic Cloud RRab and RCG blends partly reproduce bright non-canonical trends readily observed in amplitude-magnitude space (I_c versus A_{I_c}). Conversely, the larger magnitude offset between classical Cepheids and RCGs causes the latter's influence to be challenging to address. The relative invariance of a Wesenheit function's slope to metallicity (e.g., W_{Vl_c}) implies that a deviation from the trend could reveal blending and photometric inaccuracies (e.g., standardization), as blending by RCGs (a proxy of an evolved red stellar demographic) can flatten period-Wesenehit relations owing to the increased impact on less-luminous shorter-period Cepheids. That could partly explain both a shallower inferred Wesenheit function and overestimated H_0 values. A consensus framework to identify and exploit blending is desirable, as presently H_0 estimates from diverse teams are unwittingly leveraged without homogenizing the disparate approaches (e.g., no blending correction to a sizable $\simeq 0^m 3$).

Unified Astronomy Thesaurus concepts: Cepheid variable stars (218); RR Lyrae variable stars (1410); Galaxy distances (590); Stellar distance (1595); Photometry (1234); Red giant clump (1370); Hubble constant (758)

1. Introduction

Blending has been identified in ground-based observations of standard candles in globular clusters, the Galactic Bulge, galaxies, and high-resolution Hubble Space Telescope (HST) data (e.g., Majaess et al. 2012; Riess et al. 2016). Blending is defined here as arising from unresolved stars along the sightline falling within a standard candle's point-spread function (e.g., classical Cepheid), yet which remain unaccounted for when extracting photometry. The extraneous flux can result in underestimated distances, and may be challenging to address depending partly on the magnitude offset between the target (e.g., RRab or classical Cepheid) and coincident star(s) (e.g., red clump giants (RCGs), or comparatively metal-rich red horizontal branch stars). The blends investigated here arise from chance superpositions with RCGs, which are abundant in the solar neighborhood and beyond, as confirmed observationally and by stellar models. As a result the stars are employed to trace Galactic structure, characterize extinction laws, and establish stellar cluster and galaxy distances (Nishiyama et al. 2005; Grocholski et al. 2007 and references therein). As shown here, RRab and RCG blends can be identified in the amplitude-magnitude plane (e.g., I_c versus A_{I_c}), and paradoxically photometric contamination may be exploited as it can advantageously propel faint extragalactic variables into the detection threshold (Majaess et al. 2018). A key impetus of the present work is to support that assertion through simulations of RCGs grafted upon Optical Gravitational Lensing Experiment (OGLE) observations of variables in the Magellanic Clouds.

Blending's impact on remote classical Cepheids is debated (e.g., null correction to $\simeq 0^m 3$), with concerns emerging near the conclusion of the HST project to secure H_0 as the additional flux can lead to an overestimated expansion rate. For reviews and rebuttals see Section 8.5 in Freedman et al. (2001), Section 7 in Mochejska et al. (2000), and Section 8 in Mochejska et al. (2001). Since that era, additional data provide an enhanced understanding

of the important degeneracies between blending, characterizing the effect of metallicity on classical Cepheid distances, and non-standard extinction laws. A method to infer the impact of metallicity is to examine changes in the Wesenheit relation as a function of galactocentric distance, and thus abundance (Luck et al. 2011, their Figure 1). However, a problem arises owing to concurrent gradients in stellar density and surface brightness. Importantly, Stanek & Udalski (1999) and Macri et al. (2001) stressed that contamination by neighboring stars near the crowded central region of a galaxy (e.g., M101) may bias the flux of more metal-rich classical Cepheids, and could compromise determinations of the metallicity effect. Assessing whether chemical composition affects the slope (α) of the Wesenheit (W_{Vl_c}) function is critical for constraining blending. A degeneracy occurs since blending can preferentially impact shorter-period Cepheids (relative flux). In sum, the slope of the Wesenheit function may be a pertinent means for identifying blending if a given relation is insensitive to metallicity (slope and magnitude, and the latter is discussed in Section 2.2). However, Riess et al. (2009b, their Figure 12) implied that the slope of the Wesenheit (W_{Vl_c}) function is sensitive to abundance and for metal-rich classical Cepheids $\alpha \simeq -3.0$, as inferred from numerous variables spanning throughout SN-host galaxies such as NGC 1309 and NGC 3021. Majaess et al. (2011) countered that the W_{Vl_c} slope is comparatively constant across a sizable metallicity baseline ($\alpha \simeq -3.3$, $\Delta[\text{Fe}/\text{H}] \simeq 1$, their Figure 1), as established from analyzing relatively local classical Cepheids in the Large Magellanic Cloud (LMC), Small Magellanic Cloud (SMC), Milky Way, NGC 6822, and IC1613, and Majaess (2010) cited that the deviant α -results determined by Riess et al. (2009b) and Ferrarese et al. (2007, NGC 5128) arose from potentially inaccurate photometry or blending corrections. Majaess (2010) likewise relayed that the Riess et al. (2009b) classical Cepheids for NGC 1309 and NGC 3021 were too blue ($V - I_c$), and yielded a nearly negligible or negative mean reddening. Reassessments of

photometry are essential. Hoffmann et al. (2016, SH₀ES) updated the team's earlier analysis, and conveyed in their companion study (Riess et al. 2016) that a global W_{VI_c} slope of $\alpha = -3.38 \pm 0.02$ was determined, therefore presumably overturning the prior overarching hypothesis (Riess et al. 2009b, their Figure 12). The lack of consensus on this topic is further discussed in Section 2.2.

This study was inspired by the aforementioned context, in tandem with desiring to confirm that blending with ubiquitous RCGs can thrust extragalactic variables into the realm of detection. In Section 2.1 it is demonstrated that observed trends tied to LMC RRab can be reproduced in part by including contaminating flux from RCG stars (particularly the $n = 1$ overdensity). The minimal magnitude offset between the classes allows the impact of blending to be identified. That is not necessarily true for classical Cepheids (Section 2.2), and the trend is comparatively challenging to discern at remote distances owing to the uncertainties, and the analysis shifts to analyzing deviations in the slope of the Wesenheit function (e.g., a potential indicator of blending).

2. Analysis

2.1. RRab and RCG Blends

Blended RRab and RCG stars were first simulated by adopting RRab period–magnitude–amplitude relations and adding scatter (Figure 1, top). Subsequent to that, the RRab and RCG blends were better approximated by grafting the RCG magnitude (I_{RC}) directly onto OGLE Magellanic Cloud RRab observations (Soszyński et al. 2009, 2010b). A mean LMC RCG magnitude of $I_{RC} \simeq 18.2$ was adopted (Alves et al. 2002), and the revised blended magnitude (I_B) was calculated via $I_B \simeq -2.5 \log(10^{-I_0/2.5} + \sum n 10^{-I_{RC}/2.5})$, where n defines the number of RCG blends. The blended RRab amplitudes (A_B) were estimated by determining the offset between contamination added at maximum ($-0.5A_0$) and minimum ($+0.5A_0$). The $n = 1$ contamination sample was randomly inferred from 1% of the original population, and the fraction was arbitrarily scaled downward for larger n . Importantly, the analysis illustrates that the observed LMC overdensity ($I_c \simeq 17^m 8$) is sampled by RRab stars contaminated by a single RCG. The broader trend toward brighter magnitudes is reproduced by increasing the number of contaminating RCGs, although contamination can stem from a diverse stellar demographic. The pattern could be sought for in extragalactic data sets, as blended RRab and RCG stars would propel a detection $>1^m$ beyond uncontaminated RRab stars, and potentially a survey's faint-magnitude limit. Moreover, modeling can be expanded to the lightcurve where blending may be evaluated in multi-parameter and Fourier space (i.e., multiband lightcurves). Blended RRab and RCG stars would then be more confidently identified, particularly within a Wesenheit framework. Note that the decrease in RRab magnitude as a function of amplitude relays the period–magnitude–amplitude correlation.

2.2. Classical Cepheid and RCG Blends

VI_c OGLE data for classical Cepheids in the Magellanic Clouds were examined (Soszyński et al. 2008, 2010a). The blended classical Cepheid and RCG flux was evaluated assuming a mean LMC magnitude for the latter of $V_{RC} \simeq 19.2$. That was paired with

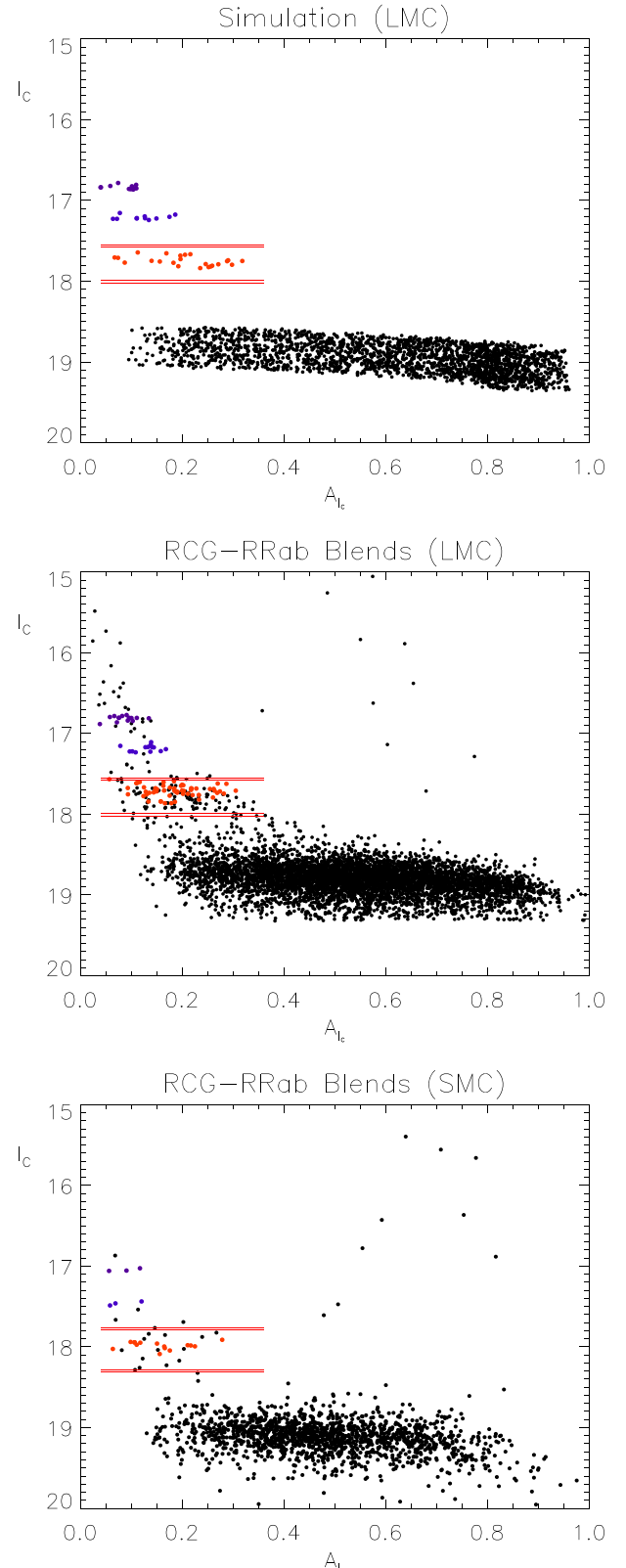


Figure 1. Blends of RRab and RCG stars (open circles) simulated from first principles (top), and grafted upon OGLE observations of the Magellanic Clouds (bottom panels). The blended stars are readily discernible in the magnitude (I_c)–amplitude (A_{I_c}) plane owing to the relatively comparable magnitudes between RRab and RCG stars, and the abundant nature of the latter. Importantly, the overdensity near $I_c \simeq 17^m 8$ is reproduced from blending by a single RCG ($n = 1$), and the brighter targets represent $n = 2, 3$.

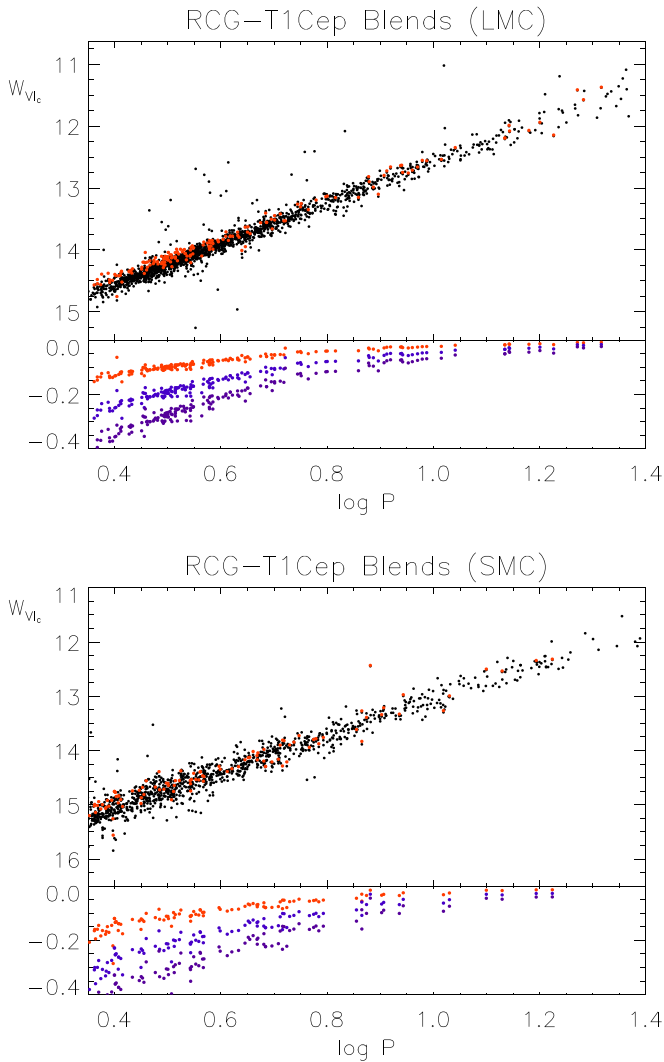


Figure 2. Simulated blends of RCGs grafted onto classical Cepheids in the Magellanic Clouds (OGLE). The blends sway the Wesenheit (W_{VI_c}) slope inferred since the impact of RCGs is relatively larger for shorter-period (less-luminous) classical Cepheids. The differentials are relayed in the bottom panels for $n = 1, 2, 3$.

the I -band estimate cited earlier to determine the contaminated Wesenheit magnitude. The blended data are conveyed in Figure 2, and represent a hypothetical remote extragalactic sample, or one sampled in a dense spiral location, or near a central region where metal-rich classical Cepheids reside. The sample was drawn randomly from 10% of the Magellanic Cloud population. The principle objective is broadly illustrating that a shallower slope can be achieved because of the larger impact of RCGs on shorter-period classical Cepheids (less luminous). In that instance the slope of an applied linear fit shifts from $\alpha \simeq -3.3$ to -3.1 (blended), and the zero-point changes by $\simeq 0^m 2$ ($n = 1$). Yet for remote dense galaxies (e.g., NGC 3370) the H-band blending corrections applied by the SH₀ES team are sizable (e.g., $> 0^m 25$), and imply that multiple RCGs could be involved in blending (see also Figure 1 in Stanek & Udalski 1999). The trends for $n = 2, 3$ are overlayed in the bottom panels of Figure 2. The blended color $V - I_c$ changes by $+ \Delta 0.02$ for $\log P \simeq 0.5$ ($n = 1$), and diminishes to relatively negligible for redder longer period LMC classical Cepheids (Figure 3). Note that the OGLE survey of the Magellanic Clouds features numerous shorter-period classical

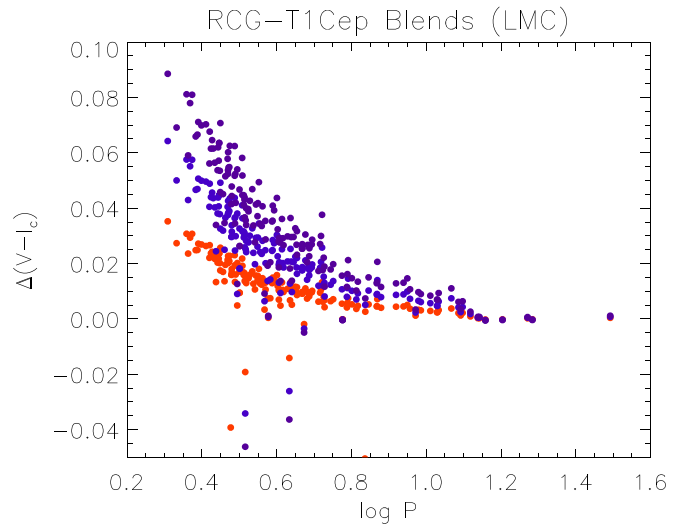


Figure 3. Impact of $n = 1, 2, 3$ RCG blends on the color ($V - I_c$) of LMC classical Cepheids.

Cepheids relative to samples of remote extragalactic variables. The latter can be restricted to a distribution of $\log P > 0.8$, owing in part to the brighter luminosity (i.e., Leavitt Law) and shifts in period owing to metallicity (Becker 1985, blue loops for $< 5 M_\odot$).

Near-infrared (NIR) Wesenheit and period-reddening relations could be viable proxies for assessing whether the photometry has been accurately corrected for photometric contamination (blending) and standardized. However, there are caveats to that assertion, one being that certain researchers advocate there is a Wesenheit zero-point magnitude dependence (W_{VI_c}) on metallicity. A brief summary is warranted, and the degeneracy with blending emerges yet again. Macri et al. (2006) applied a suite of criteria aiming to mitigate blending (e.g., their Figure 17), and subsequently argued that HST data for classical Cepheids spanning M106 (metal-rich central region to the metal-poor periphery) implied a metallicity effect of $\gamma = -0.29 \pm 0.16 \text{ mag dex}^{-1} (VI_c)$. However, Majaess (2010) underscored that the revised Riess et al. (2009b) abundance gradient for M106 implies that the Macri et al. (2006) result nearly doubles to an unrealistic value (see also Bresolin 2011, and Section 5 in Macri et al. 2001), and consequently blending remained a key factor. Yet Shappee & Stanek (2011) and Gerke et al. (2011) favored a sizable VI_c metallicity dependence of $\gamma = -0.80 \pm 0.21 \text{ mag dex}^{-1}$ and $-0.62 \pm 0.33 \text{ mag dex}^{-1}$ accordingly, namely after examining HST and Large Binocular Telescope data for classical Cepheids at varying galactocentric radii in M101 and M81. Majaess et al. (2011) disagreed with those conclusions and advocated that photometric contamination was the contributor, since applying such an immense metallicity dependence yielded anomalous results for the distances to the comparatively nearby Magellanic Clouds (e.g., $\mu_{0,\text{LMC}} \neq 18.1$). Indeed, Majaess et al. (2011) reiterated that the impact of metallicity could be evaluated on the basis of several methods that did not rely exclusively on an uncertain multi-degenerate galactocentric approach, and that W_{VI_c} observations of classical Cepheids were comparatively insensitive to chemical composition. Therefore, direct empirical constraints on blending stem partially from tracking the W_{VI_c} magnitude changes of classical Cepheids throughout a galaxy (i.e., from the low stellar-density periphery to near the crowded core). Crucially, Riess et al. (2009a) constructed a preliminary multiband

procedure to apply blending corrections, and then partly ascertained from galactocentric analyses of numerous spiral galaxies that $\gamma = -0.27 \pm 0.18 \text{ mag dex}^{-1}$ (W_{H,Vl_c}). That was subsequently substantially reduced by half to $\gamma = -0.14 \pm 0.06 \text{ mag dex}^{-1}$ (Riess et al. 2016), and for W_{Vl_c} the SH₀ES team argued for $\gamma = -0.20 \pm 0.05 \text{ mag dex}^{-1}$. The present SH₀ES approach requires revision if indeed the metallicity corrections at W_{H,Vl_c} and W_{Vl_c} are relatively negligible (Majaess et al. 2011, see also Bono et al. 2010).

Lastly, the blended classical Cepheid and RCG Wesenheit magnitude (Figure 2) was computed using an extinction law commonly employed by the OGLE team of $R_{Vl_c} = A_V/E(V-I_c) \simeq 2.55$. However, $R_{Vl_c} = 2.45$ is utilized too, and the overall topic shall be discussed at length elsewhere. There could exist both a mean extinction law offset between the calibration and target samples, and variations within each set. For broader context, note that the Galactic Bulge sightline may be characterized by an anomalous R_{Vl_c} extinction law relative to the Galactic Disk (Udalski 2003). However, O-stars examined by Majaess et al. (2016) indicate the disk along the Galactic Bulge sightlines adheres to a canonical $R_{V,BV}$, yet an anomalous visual extinction law characterizes the Carina sightline (Turner 2012; Majaess et al. 2016). The transition to given longer wavelengths mitigates that problem (Freedman et al. 2012; Majaess et al. 2016), but contaminating flux from RCGs (and red evolved stars) may increase. The Wesenheit function's nearly reddening free nature is advantageous, but a disadvantage emerges since the uncertainty stemming from the extinction law is magnified by a significant color term. Additional research on the topic is desirable.

3. Conclusion

Blending was investigated as it relates to RCGs contaminating RRab stars and classical Cepheids. The former are abundant, and certain trends in OGLE RRab data were explained by contaminating the photometry with a single RCG (i.e., LMC overdensity near $I_c \simeq 17^m 8$, Figure 1). The brighter blends are readily identified (I_c versus A_{I_c}) in part owing to the relatively marginal magnitude offset between RRab and RCG stars. The assertion that blending may advantageously cause variable stars to be detectable in more remote galaxies was confirmed.

The larger magnitude offset between RCGs and classical Cepheids complicates the identification of that pairing. The slope of the Wesenheit function (e.g., W_{Vl_c}) can be valuable for identifying those blended cases and inaccurate photometry, since shorter-period classical Cepheids are acutely impacted by contamination (Figure 2), and if a given Wesenheit relation is comparatively insensitive to metallicity (Majaess et al. 2011, their Figure 1). Figure 2 illustrates the slope (α) can change to lower values as a result of blending by RCGs (e.g., $|\Delta\alpha| \simeq 0.3$, $n = 2$), and the RCG class provides a broader view of the contamination an evolved red demographic can impose (e.g., asymptotic giant branch (AGB) stars, red giants).

An important broader objective remains securing a reliable H_0 and thus further constraining cosmological models. Investigations into the impact of blending are key to achieving that goal, as evidenced by the debate pertaining to whether the SH₀ES and CHP teams yielded an H_0 ($\simeq 74 \text{ km s}^{-1} \text{ Mpc}^{-1}$) offset from the Planck framework ($H_0 = 67.4 \pm 0.5$: $\text{km s}^{-1} \text{ Mpc}^{-1}$). The topic gained momentum in part since the authors of Tamman & Sandage (2010) are no longer present to argue

for $H_0 = 62.3 \pm 5 \text{ km s}^{-1} \text{ Mpc}^{-1}$ (see also Turner 2014).³ Nonetheless, Freedman et al. (2019; Carnegie-Chicago Hubble Program (CCHP)) subsequently revised their value downward to $H_0 = 69.8 \pm 1.9 \text{ km s}^{-1} \text{ Mpc}^{-1}$, hence reducing the tension relative to the CMB result. A follow-up study by Yuan et al. (2019, SH₀ES) argued that Freedman et al. (2019) neglected blending and a standardization offset when determining the tip of the red giant branch (TRGB) absolute magnitude, and consequently their H_0 (TRGB+SNe Ia) should be increased back upward to $72.4 \pm 2.0 \text{ km s}^{-1} \text{ Mpc}^{-1}$, and thereby bolstering the SH₀ES perspective. Yet the counter effect should likewise be considered, namely the impact of blending on remote targets in all the following, concurrently: the HST key project to determine H_0 sample (Gibson et al. 2000; Freedman et al. 2001), the CHP mid-IR Spitzer classical Cepheid observations (Freedman et al. 2012), the Freedman et al. (2019, CCHP) set, and the Sandage et al. (2006) data. That may in sum reduce H_0 and supersede presently quoted uncertainties ($0^m 04$), since separate teams did not account for blending in a similar fashion to Riess et al. (2009a, or Riess et al. 2016). Indeed, efforts to strengthen and compare H_0 estimates should include an assessment of how contamination linked to remote targets is addressed. Riess et al. (2009a) applied significant average photometric contamination corrections (H -band), and Riess et al. (2016) note that the median blending shift tied to SN-host galaxies is $0^m 18$. However their procedure should be independently scrutinized in concert with the systematic uncertainties flowing from the remote blending corrections applied. The HST project did not apply similar corrections for photometric contamination, but provided a sizable uncertainty and elaborate discussion tied to the phenomenon (e.g., Freedman et al. 2001 and references therein). H_0 estimates could likewise be improved by inevitably pairing validated Gaia, Hipparcos (HIP), and HST parallaxes for classical Cepheids with a subset of cluster Cepheids where consensus exists (e.g., Turner et al. 2012; Groenewegen 2018; Riess et al. 2018; Shanks et al. 2019 and references therein), and/or via an NIR universal Wesenheit template (Majaess et al. 2011 and references therein). The resulting analysis in tandem with other approaches may facilitate the breaking of key degeneracies, and for benchmarking the slope of the Wesenheit function, the impact of metallicity, blending, and the distance to the LMC and M106 (pending the availability of viable and independently attested blending-corrected photometry for the latter). Indeed, multiple quantities may require adjustment that conspire to sway H_0 unidirectionally, and narrowing the focus may inadvertently mask a broader problem. The dawn of precision cosmology seemingly occurs in an era where a lack of agreement exists concerning fundamentals associated with the Leavitt Law, owing in part to degeneracies (e.g., blending, metallicity, and extinction law).

D.M. is grateful to the following consortia and individuals whose efforts or advice helped foster the research: OGLE, CDS, arXiv, NASA ADS, (C)CHP, SH₀ES, D. Minniti, & D. Turner.

³ Admittedly, Majaess (2010) relayed that a hybrid Galactic classical Cepheid calibration tied to cluster Cepheids and HST parallaxes implied that the Sandage et al. (2006) classical Cepheid distances were too remote, and yielded an artificially low H_0 (see also van Leeuwen et al. 2007). However that team did not apply blending corrections (e.g., Riess et al. 2009a) which would shift H_0 in the opposite direction.

References

- Alves, D. R., Rejkuba, M., Minniti, D., & Cook, K. H. 2002, *ApJL*, **573**, L51
 Becker, S. 1985, in IAU Coll. 82, Cepheids: Theory and Observation, ed. B. F. Madore (New York: Cambridge Univ. Press), 104
 Bono, G., Caputo, F., Marconi, M., et al. 2010, *ApJ*, **715**, 277
 Bresolin, F. 2011, *ApJ*, **729**, 56
 Ferrarese, L., Mould, J. R., Stetson, P. B., et al. 2007, *ApJ*, **654**, 186
 Freedman, W. L., Madore, B. F., Gibson, B. K., et al. 2001, *ApJ*, **553**, 47
 Freedman, W. L., Madore, B. F., Hatt, D., et al. 2019, *ApJ*, **882**, 34
 Freedman, W. L., Madore, B. F., Scowcroft, V., et al. 2012, *ApJ*, **758**, 24
 Gerke, J. R., Kochanek, C. S., Prieto, J. L., et al. 2011, *ApJ*, **743**, 176
 Gibson, B. K., Stetson, P. B., Freedman, W. L., et al. 2000, *ApJ*, **529**, 723
 Grocholski, A. J., Sarajedini, A., Olsen, K. A. G., et al. 2007, *AJ*, **134**, 680
 Groenewegen, M. A. T. 2018, *A&A*, **619**, A8
 Hoffmann, S. L., Macri, L. M., Riess, A. G., et al. 2016, *ApJ*, **830**, 10
 Luck, R. E., Andrievsky, S. M., Kovtyukh, V. V., et al. 2011, *AJ*, **142**, 51
 Macri, L. M., Calzetti, D., Freedman, W. L., et al. 2001, *ApJ*, **549**, 721
 Macri, L. M., Stanek, K. Z., Bersier, D., et al. 2006, *ApJ*, **652**, 1133
 Majaess, D. 2010, *AcA*, **60**, 121
 Majaess, D., Dékány, I., Hajdu, G., et al. 2018, *Ap&SS*, **363**, 127
 Majaess, D., Turner, D., Dékány, I., Minniti, D., & Gieren, W. 2016, *A&A*, **593**, A124
 Majaess, D., Turner, D., & Gieren, W. 2011, *ApJL*, **741**, L36
 Majaess, D., Turner, D., & Gieren, W. 2012, *PASP*, **124**, 1035
 Mocchejska, B. J., Macri, L. M., Sasselov, D. D., et al. 2000, *AJ*, **120**, 810
 Mocchejska, B. J., Macri, L. M., Sasselov, D. D., et al. 2001, arXiv:[astro-ph/0103440](#)
 Nishiyama, S., Nagata, T., Baba, D., et al. 2005, *ApJL*, **621**, L105
 Riess, A. G., Casertano, S., Yuan, W., et al. 2018, *ApJ*, **861**, 126
 Riess, A. G., Casertano, S., Yuan, W., et al. 2019, *ApJ*, **876**, 85
 Riess, A. G., Macri, L., Casertano, S., et al. 2009a, *ApJ*, **699**, 539
 Riess, A. G., Macri, L., Li, W., et al. 2009b, *ApJS*, **183**, 109
 Riess, A. G., Macri, L. M., Hoffmann, S. L., et al. 2016, *ApJ*, **826**, 56
 Sandage, A., Tammanne, G. A., Saha, A., et al. 2006, *ApJ*, **653**, 843
 Shanks, T., Hogarth, L. M., & Metcalfe, N. 2019, *MNRAS*, **484**, L64
 Shappee, B. J., & Stanek, K. Z. 2011, *ApJ*, **733**, 124
 Soszyński, I., Poleski, R., Udalski, A., et al. 2008, *AcA*, **58**, 163
 Soszyński, I., Poleski, R., Udalski, A., et al. 2010a, *AcA*, **60**, 17
 Soszyński, I., Udalski, A., Szymański, M. K., et al. 2009, *AcA*, **59**, 1
 Soszyński, I., Udalski, A., Szymański, M. K., et al. 2010b, *AcA*, **60**, 165
 Stanek, K. Z., & Udalski, A. 1999, arXiv:[astro-ph/9909346](#)
 Tammanne, G. A., & Sandage, A. 2010, *ApSSP*, **15**, 289
 Turner, D. G. 2012, *Ap&SS*, **337**, 303
 Turner, D. G. 2014, AAS Meeting, **224**, 318.09
 Turner, D. G., Majaess, D. J., Lane, D. J., et al. 2012, *MNRAS*, **422**, 2501
 Udalski, A. 2003, *ApJ*, **590**, 284
 van Leeuwen, F., Feast, M. W., Whitelock, P. A., et al. 2007, *MNRAS*, **379**, 723
 Yuan, W., Riess, A. G., Macri, L. M., et al. 2019, *ApJ*, **886**, 61